



Effect of Al₂O₃ Doping on Antibacterial Activity of 45S5 Bioactive Glass

Yeliz Başaran Elalmış^{1*}  

¹Yildiz Technical University, Faculty of Chemical and Metallurgical Engineering, Department of Bioengineering, 34220, Istanbul, Turkey.

Abstract: 45S5 bioactive glasses (BGs) are special class of glasses that form chemical bonds with surrounding bone tissue, which is due to the dissolution behavior of these glass materials. Furthermore, BG shows an antibacterial effect since the dissolution of BG results with high aqueous pH that affect bacterial viability. In this study, the antibacterial activity of Al₂O₃ doped bioactive glasses (AGs) was evaluated. AGs were produced via the melt quenching method. Functional groups of glasses were evaluated with Fourier Transform Infrared (FTIR) analysis, and glassy structure was evaluated by X-ray diffraction (XRD). Specific surface area, particle size information, and density of milled BG and AGs were obtained using surface area and porosity instrument, laser scattering particle size distribution analyzer and He pycnometer, respectively. Antibacterial activity of bioactive glasses was investigated on *Staphylococcus aureus* and *Escherichia coli* via Standard Colony Count Method at 50 mg/mL concentration and different time points, pH change of the media in the presence of BG and AGs at 50 mg/mL concentration was also measured at identical time points. XRD analysis revealed amorphous structure of BG and AGs. Similar specific surface area, particle size and density values were obtained for BG and produced AGs. Antibacterial test results showed that Al₂O₃ doped 45S5 bioactive glasses had decreased antibacterial activity compared to 45S5 bioactive glass for both bacteria studied.

Keywords: Bioactive glass, Al₂O₃ doped bioactive glass, antibacterial activity.

Submitted: December 04, 2020. **Accepted:** February 08, 2021.

Cite this: Başaran Elalmış Y. Effect of Al₂O₃ Doping on Antibacterial Activity of 45S5 Bioactive Glass. JOTCSA. 2021; 8(2):419-28.

DOI: <https://doi.org/10.18596/jotcsa.835912>.

***Corresponding author. E-mail:** elalmis@yildiz.edu.tr.

INTRODUCTION

Materials that have been designed to yield particular biological activity are generally described as bioactive materials. By definition a bioactive material is a material that undergoes significant surface reactions after implantation and lead to hydroxyapatite (HA)-like layer formation, responsible for firm tissue bonding (1). Bioactive glass (BG) which is commonly constituted of SiO₂, CaO, P₂O₅, and Na₂O is a special type of glass system (2). This silicate glass is based on SiO₂ network which forms the 3D glass. Low SiO₂ content in comparison with more durable silicate glasses, high glass network modifier (Na₂O and CaO) content, and high CaO:P₂O₅ ratio are the key properties of 45S5 glass which lead to the bioactivity (1).

Fibrous tissue surrounds the artificial materials after implantation into bone defects. However, Hench and coworkers discovered in 1971 that Bioglass® (in Na₂O-CaO-SiO₂-P₂O₅ system) does not lead to fibrous tissue formation, instead contact and form firm chemical bonds with surrounding bone tissue (3). Frequently used silicate BGs form a bone like HA layer which is fundamental for strong bone-material interfacial bonding. Bioactivity and bone bonding mechanism mostly for 45S5 Bioglass® has been broadly studied (*in vitro* and *in vivo*), degradation of biomaterials and subsequent HA layer formation on their surface provides the bonding ability of glass and glass-ceramics. Formed surface HA layer mimics the mineral composition of bone (4). Osteoblasts produce collagen fibrils at the interface and hydroxycarbonated apatite (HCA) crystals bond to this collagen fibrils, which creates a firm chemical interface. HA layer formation is a result of chemical

reaction series on the implant surface when contact with the bodily fluids (5). Following successive steps are involved in this series of reactions. Ion dissolution from BG structure into the medium takes place during the 1st step. 2nd step involves the reaction between dissolved Ca²⁺ and (PO₄)³⁻ ions, and subsequent amorphous calcium phosphate (ACP) precipitation. ACP growth is induced during the 3rd step due to the pH instability and increased ion dissolution, and finally incorporation of media (OH)⁻ and (CO₃)²⁻ ions to the ACP layer, and crystallization as HA layer takes place during the 4th step (4). Briefly, reactions taking place on the surface of the bioactive silicate glass (for instance 45S5 Bioglass[®]) material and following cellular reactions lead to the bonding to the living bone tissue. Furthermore, release and substitution of crucial concentrations of soluble Si, Ca, P and Na ions lead to the favorable extracellular and intracellular reactions that rapidly promote bone formation (6).

Bone regeneration ability of 45S5 BG has led to its wide clinical use as bone filling material. Furthermore, it was stated that BG could enhance healing of wounded soft tissue. Prevention of infection during the healing of wounded skin is a crucial matter. Usually, in clinic antibiotics are used against infection. Thus, wound dressing materials that enhance the healing of the wound and show antibacterial activity as well would be useful (7). BG antibacterial activity was attributed to be mainly due to the high pH and osmotic effects which are caused by alkali ion release from the BG and non-physiological silica, sodium and calcium concentrations (7, 8).

Glass materials that are planned to be used as implants in the human body must have solubility to a certain degree to be able to attach to the tissue. These glasses are bioactive and they contain SiO₂ less than around 60%, higher SiO₂ contents lead to decreased solubility so that the surface reactions required for the bioactivity cannot take place (9). In the case of long term implants decreased solubility without bioactivity loss may be practical (10). Glass solubility reduction can be provided via increasing silica content, or decreasing modifier content, or adding multivalent cations. Generally, alumina is considered as glass structure stabilizer due to its non-bridging oxygen elimination behavior. In addition to this, dissolution is also retarded by surface alumina silicate film formation (9).

Al₂O₃ addition to glass is the conventional way of glass solubility control. However, the addition of alumina may have an inhibitory effect on bone

bonding. It was found in a previously reported study that Al₂O₃ at 1.5 wt% could be added with no interference to mineralization of osteoid (11). Bioactive glasses with high Al₂O₃ content (1.5-2.5 mol%) were reported to show cytotoxic effect on human osteosarcoma U2-OS cells (12).

In this study, 45S5 bioactive glasses with 1 and 2 wt % Al₂O₃ content were prepared. The antibacterial effect of prepared Al₂O₃ doped bioactive glasses and 45S5 bioactive glass (Bone-G Active[®], Meta Bioengineering and R&D Services Inc., Turkey) was evaluated on *Escherichia coli* and *Staphylococcus aureus* in relation with the changes in pH.

EXPERIMENTAL SECTION

Materials

Aluminum oxide and silicon dioxide (quartz) were from Riedel de Haën (Sigma-Aldrich Laborchemikalien GmbH, Seelze, Germany). CaCO₃, Na₂HPO₄·2H₂O, and NaHCO₃ were obtained from Merck Chemicals (Darmstadt, Germany). 45S5 bioactive glass (Bone-G Active[®]) was obtained as a gift sample from Meta Bioengineering and R&D Services Inc., Turkey. *Escherichia coli* (ATCC 25922) and *Staphylococcus aureus* (ATCC 25923) used in this study were from the American Type Culture Collection. Media and chemicals used in the microbial testing were obtained from Sigma-Aldrich.

Production of bioactive glass and alumina doped bioactive glass materials

To produce melt-derived alumina doped 45S5 bioactive glasses a mixture of SiO₂, NaHCO₃ as source of Na₂O, CaCO₃ as source of CaO, Na₂HPO₄·2H₂O as sources of Na₂O and P₂O₅, and Al₂O₃ were melted in predetermined amounts. Bone-G Active[®] and produced Al₂O₃ doped glasses and their compositions are given in Table 1. Al₂O₃ doped bioactive glasses were produced according to a previously reported method (13, 14). Briefly, raw materials were first weighed, homogeneously mixed, and melted in a platinum crucible at 1400 °C, and then quenched into the water at room temperature. Glassy particles were dried and crushed for homogeneity, melted again (1450 °C, 2 hours) and poured into the casting plate. Production process was completed by the annealing of the bioactive glasses in an oven at 550 °C. Bone-G Active[®] and prepared bioactive glasses were crashed and subsequently ground to powder using a planetary ball mill (PM 400, Retsch GmbH, Haan, Germany). Bone-G Active[®] was abbreviated as BG, and produced 1 wt% Al₂O₃ doped 45S5 as AG1, and 2 wt % Al₂O₃ doped 45S5 as AG2.

Table 1: Bioactive glasses and their compositions.

Glass	Composition	Description
BG	SiO ₂ 45 wt%, Na ₂ O 24.5 wt%, CaO 24.5 wt% and P ₂ O ₅ 6 wt%	Bone-G Active®
AG1	SiO ₂ 45 wt%, Na ₂ O 24.5 wt%, CaO 23.5 wt%, P ₂ O ₅ 6 wt% and Al ₂ O ₃ 1 wt%	1 wt% Al ₂ O ₃ doped 45S5 glass
AG2	SiO ₂ 45 wt%, Na ₂ O 24.5 wt%, CaO 22.5 wt%, P ₂ O ₅ 6 wt% and Al ₂ O ₃ 2 wt%	2 wt% Al ₂ O ₃ doped 45S5 glass

Characterization of produced bioactive glass and Al₂O₃ doped bioactive glasses

Functional groups of glass structures were evaluated using a Fourier transform infrared spectrometer (FTIR, Shimadzu, IR Prestige 21) in the wavenumber range of 2000–650 cm⁻¹ and 4 cm⁻¹ resolution. X-Ray diffractions of BG, AG1 and AG2 obtained with Rigaku D/Max-2200 Ultima diffractometer (40kV, 30mA) using CuK α radiation source in the 2 θ range of 10–90° with 0.08° step size. Specific surface area of BG, and produced AG1 and AG2 samples was determined at 77 K by N₂ adsorption with the use of a surface area and porosity instrument (Micromeritics, TriStar II). Samples were outgassed prior to analysis at 90°C for 1 h and 250°C for 2 hours under N₂ flow. Specific surface area was calculated using Brunauer-Emmett-Teller (BET) method (0.05 < p/po < 0.30). Particle size distribution of BG, AG1 and AG2 powders was evaluated using laser scattering particle size distribution analyzer (Horiba, LA-350), and density of glass powders was measured using helium pycnometer (Thermo Scientific, Pycnomatic ATC).

Antibacterial activity of 45S5 bioactive glass and alumina doped bioactive glasses

In this study two classic bacteria, Gram-positive *Staphylococcus aureus* (*S.aureus*, ATCC25923), and Gram-negative *Escherichia coli* (*E.coli*, ATCC25922) were used to investigate bactericidal activity. The antimicrobial tests were performed using the modified American Standard ASTM E2149-01 method (15), in which samples are stirred constantly in bacterial suspension and thus, ensure good contact between the sample and the bacteria (16). *S.aureus* and *E.coli* were incubated at 37°C overnight, and preserved on nutrient plates. Concentrations of bacterial solution were standardized using the relationship between absorbance at 590 nm (OD590) and colony forming units (CFU) per milliliter determined by the plate count method. 100 mL of *E.coli* or *S.aureus* suspension prepared in 0.1 M aqueous phosphate buffered saline (pH 7.0, 10¹¹ cells/mL) was added into the sterile Erlenmeyer flasks containing 50 mL of nutrient broth. Bacteria were suspended with the addition of 10 mL saline solution (0.9% NaCl) to obtain approximately 10⁶ CFU/mL, prior to the antibacterial testing. Variation in antibacterial activity depending on the bioactive glass type was determined using 50 mg/mL BG, AG1 or AG2. Bioactive glass powders were added in to 1 mL of

bacterial suspension and antibacterial activity was determined after 0 min, 10 min, 1 h, 6h, and 24 h of incubation for both bacteria. 10 μ L of bacterial suspension was taken after above-mentioned incubation times and plated on nutrient agar plates overnight. The colonies formed were counted via Standard Colony Count Method and antibacterial activity was calculated using Eq. 1 (17). Bacterial solution without bioactive glass powders was used as control.

$$AA (\%) = \frac{(C_{Control} - C_{survivor})}{C_{control}} \times 100 \quad (\text{Eq. 1})$$

Where, AA is antibacterial activity, C_{control} is cell count of control and C_{survivor} is the survivor count of test.

pH measurements

BG, AG1 and AG2 particles were added into flasks containing 5 mL nutrient broth medium at concentration of 50 mg/mL. After stirring for 1 min, the solutions were placed at 37 °C for 24 hours. The pH values of the media were measured at certain time points (i.e., 0 min, 10 min, 1 h, 6 h, and 24 h).

RESULTS AND DISCUSSION

Characterization of bioactive glasses

FTIR spectra of milled BG, AG1 and AG2 powders are presented in Figure 1. Main absorption bands identified in the FTIR spectra were around 738 cm⁻¹, 866 cm⁻¹, 910 cm⁻¹, 1005 cm⁻¹, and 1454 cm⁻¹ for the prepared glass powders. The bands present around 738 cm⁻¹ in the FTIR spectra of BG, AG1 and AG2 were attributed to the bending mode of Si-O-Si, characteristic for silicate materials containing non-bridging oxygen atoms. Stretching vibrations of SiO₄ and PO₄ are generally assigned to the broad and strong intensity band observed between 800 and 1300 cm⁻¹ (18). Strong absorption peak around 1005 cm⁻¹ can be attributed to the asymmetric stretching vibrations of Si-O-Si bridging oxygen atoms, the absorption peak at 910 cm⁻¹ and shoulder at 866 cm⁻¹ (missing in the AG2 FTIR spectra) were attributed to Si - O stretching which were due to the presence of non-bridging oxygen atoms (18-20). Small peak around 1454 cm⁻¹ was due to the ionic carbonate groups adsorbed on the bioactive glass surfaces (19, 21).

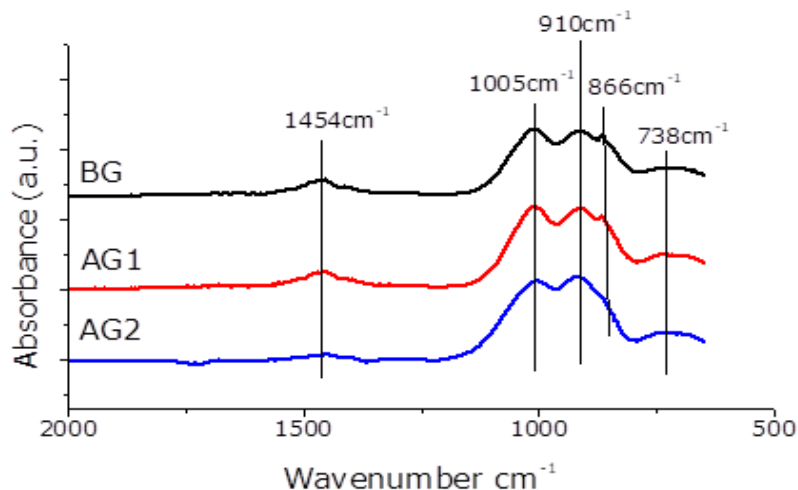


Figure 1: FTIR spectra of BG, AG1, and AG2.

XRD patterns of BG, AG1, and AG2 are presented in Figure 2. As seen, the crystalline peaks were absent in XRD patterns of the bioactive glass samples. However, a broad peak around $2\theta=30^\circ$ which

indicates the amorphous structure typical for glassy phases (22) was observed in XRD patterns of the BG, AG1, and AG2.

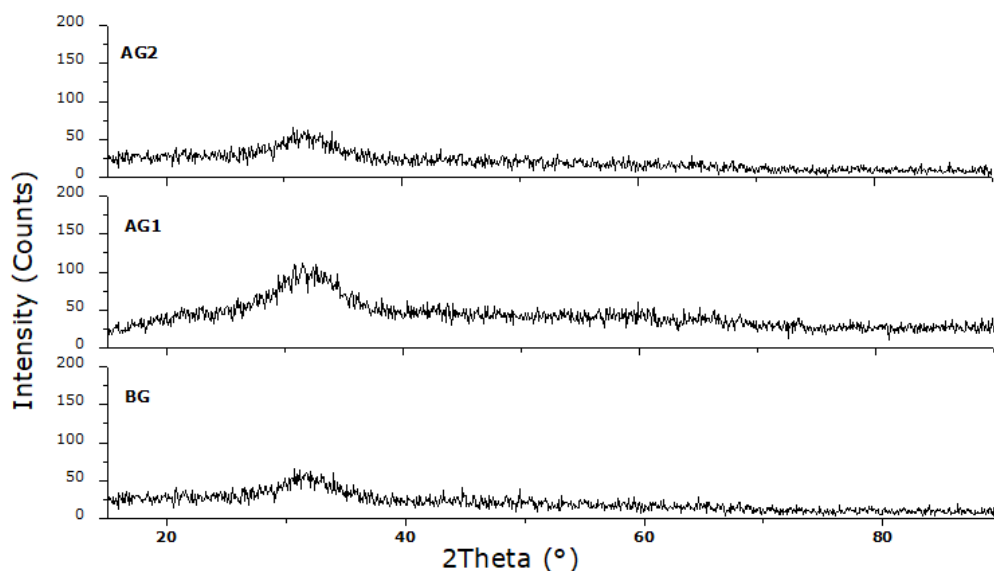


Figure 2: XRD patterns of BG, AG1 and AG2.

BG and produced melt-derived AG1 and AG2 were ground into powder using planetary ball mill prior to antibacterial tests. Specific surface area (S_{BET}), particle size information and density values of milled BG, AG1, and AG2 are presented in Table 2 and particle size distributions of BG, AG1 and AG2 are

given in Figure 3. As can be seen from the results presented surface area, particle size and density values of BG, AG1, and AG2 powders were similar, which is attributed to be highly dependent on the glass production method and subsequently applied milling process.

Table 2: Specific surface area (S_{BET}), particle size information and density values of BG, AG1, and AG2

Sample	S_{BET} (m ² /g)	Particle size information		Density (g/cc)
		$D_{0.5}$ (μm)	Span	
BG	0.76	13.98	3.73	2.70
AG1	0.82	13.99	4.49	2.65
AG2	1.07	14.33	5.75	2.63

Antibacterial activity of the glass is essentially dependent on its composition. Since, it effects the ion release rate and consequently the pH and

osmolality of the media which have central effect on the antibacterial activity. Particle size, surface area, porosity, and morphology properties of the glass

materials can also influence their antibacterial activity (4). Additionally, this activity is dependent on the glass concentration and tested microorganism (23). Silicate network dissolution rate is effected by the particle size of the powder so that the rate of dissolution increases with the decrease in particle size (22). In this study, BG and produced AG1 and AG2 glasses were milled at certain conditions to obtain glass powders with similar

particle size to eliminate the potential effect of particle size on the ion release. Since the aim of the study was to evaluate the antibacterial activity on the bacteria studied depending on the Al_2O_3 content of the glasses, surface area was also determined, which is also stated to play an important role in glass dissolution and accordingly antibacterial activity of milled glass powders.

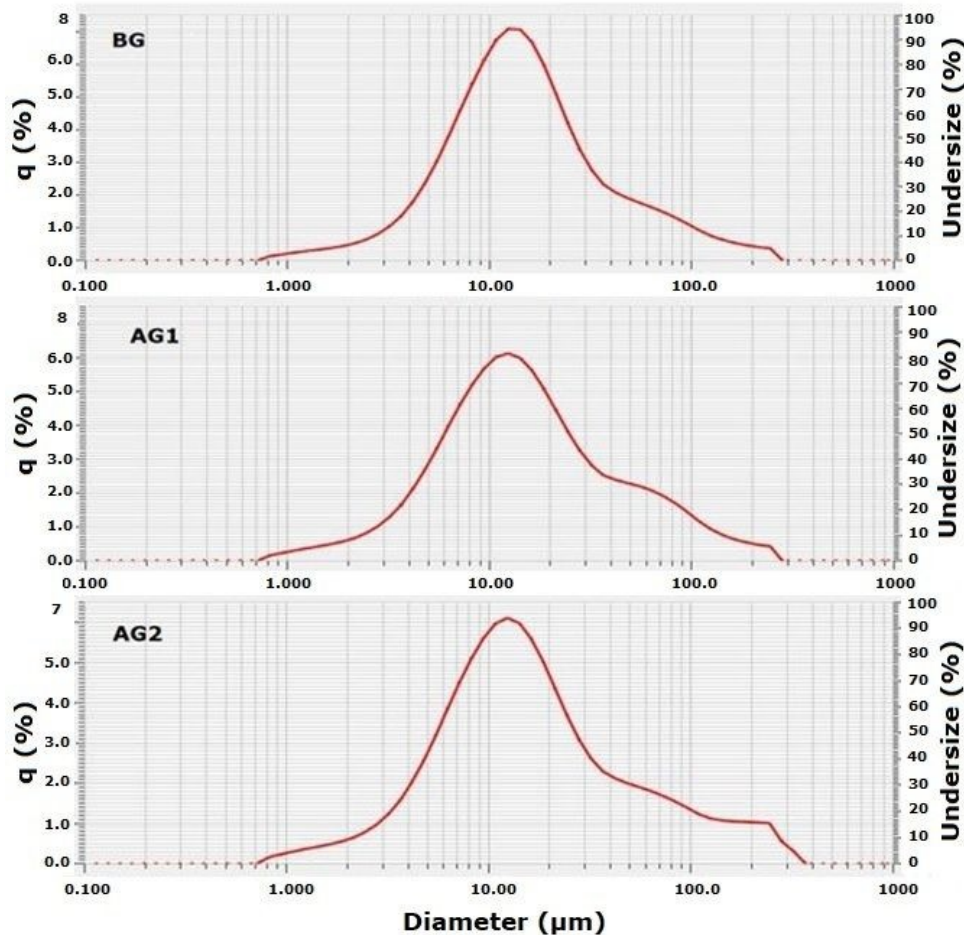


Figure 3: Particle size distributions of BG, AG1, and AG2.

Antibacterial Activity of Bioactive Glasses, and pH Changes

Antibacterial activity of BG, AG1, and AG2 at 50 mg/mL concentration was determined at different time points (i.e. 0 min, 10 min, 1h, 6 h, and 24 h) as may be seen in Fig. 4. BG exhibited antibacterial effect against two pathogenic bacteria at 6th hour with

bactericidal percentages of 42% and 46% for *E.coli* and *S.aureus*, respectively. On the other hand, at 6th hour AG1 exhibited antibacterial effect with bactericidal percentage of 20% on *S.aureus* only. AG2 did not exhibit antibacterial effect at 6th hour on both bacteria.

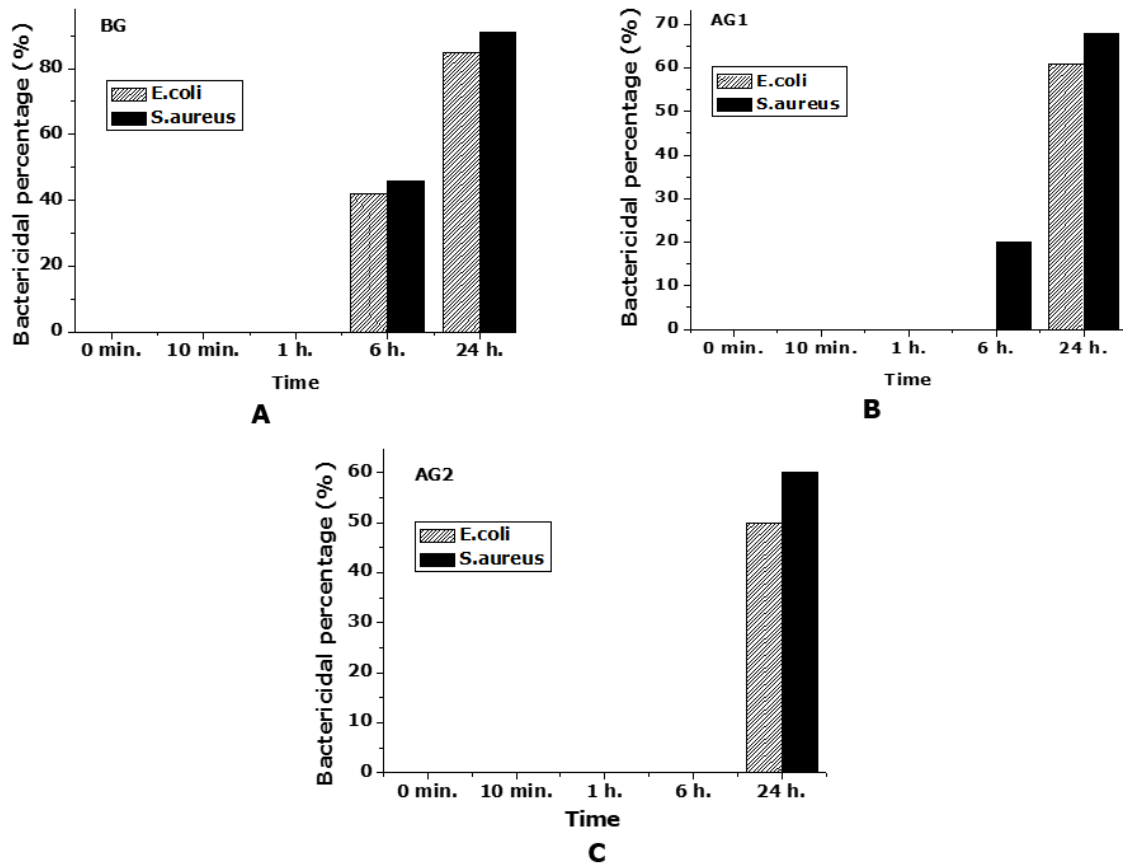


Figure 4: Bactericidal percentages of A) BG, B) AG1, and C) AG2 at concentrations of 50 mg/mL depending on time.

It was observed that antibacterial effect of BG and produced Al_2O_3 doped bioactive glasses (AG1 and AG2) was in the BG>AG1>AG2 order after 24 hours of incubation for both bacteria (Fig. 5). BG showed

91% antibacterial effect against *S.aureus* and 85% antibacterial effect against *E.coli* after 24 hours of incubation.

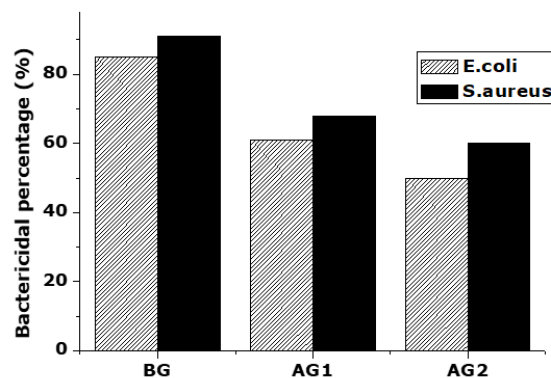


Figure 5: Bactericidal percentages of BG, AG1, and AG2 after 24 h of incubation at bioactive glass concentrations of 50 mg/mL.

The aqueous pH values of 50 mg/mL BG, AG1 or AG2 containing suspensions increased with incubation time as seen in Figure 6. 0 time point represented the pH of the nutrient broth media before the addition of bioactive glass samples. pH value of the BG containing media increased from 7.1 to 8.4 in the first hour, in contrast there was no significant difference in pH values of AG1 and AG2

containing suspensions in the first hour. pH values of BG, AG1, and AG2 containing suspensions were 9.1, 8.2, and 7.9 at the 6th hour, respectively. pH increase of BG and produced Al_2O_3 doped bioactive glass containing broth displayed the order of BG>AG1>AG2 after 24 hours of incubation. 45S5 bioactive glass (BG) showed pH values clearly higher than the alumina doped glasses (Fig. 6). The change

observed in aqueous pH values of the BG, AG1, and AG2 containing suspensions was in accordance with

the bactericidal behavior of these bioactive glass samples.

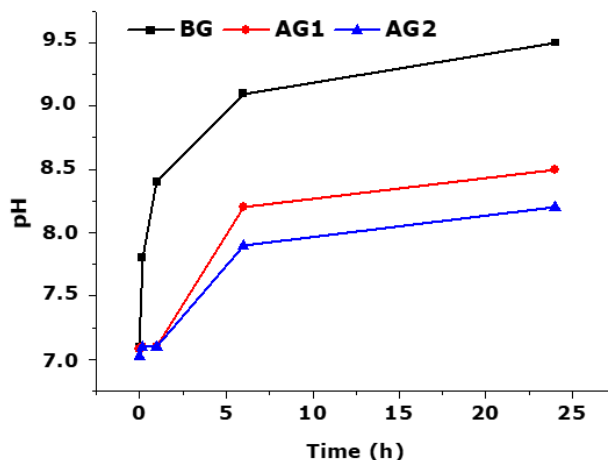


Figure 6: pH change depending on incubation time.

Antibacterial effect of bioactive glasses was mainly attributed to the high pH values resulting from the alkali ion release from the bioactive particles, in previous reports (7, 24-25). Reaction series taking place on the bioactive glass surface in aqueous media such as, soluble silica, calcium, and sodium release, led to an increased pH value (7). Zhang et al. (24) reported that higher glass dissolution tendency lead to higher increases in solution pH and alkali ions concentrations, which results with better antibacterial activity of the glass. Thus, mechanism of dissolution of bioactive glasses is crucial in the evaluation of glass antibacterial activity, and high antibacterial activity glasses are probably glasses with high dissolution rate (24).

Increase in nutrient broth pH in the presence of Al₂O₃ doped bioactive glasses, AG1 and AG2, was significantly low compared to nutrient broth pH increase containing traditional 45S5 bioactive glass BG. This is probably due to the elimination of some non-bridging oxygen by Al₂O₃, which decreases the solubility of the glass (5).

Alkaline ion release, specially Ca²⁺ ions, and increase in medium pH cause the antibacterial activity of glass-ceramic and glass materials. Ion release increase the osmolarity and the pH, leading to unbalanced bacterial intracellular Ca²⁺, depolarizes the bacterial cell membrane and subsequently kills the bacterial cells. Thus antibacterial activity of these materials is dependent on the rate of ion release in aqueous media (4). Consequently, bioactive glass antibacterial activity mechanism probably depends on the combination of parameters, which include glass network dissolution caused osmotic effect and high pH, and also network-modifying ions (26).

CONCLUSION

The following conclusion was reached within the limitations of this study, which is on the effect of

alumina doping on antibacterial activity of 45S5 bioactive glass. Alumina addition to 45S5 bioactive glass structure resulted in decreased antibacterial activity and decreased the pH increment which was regarded to be associated with decreased ion dissolution from glass structure. Alumina is considered as glass structure stabilizer due to its non-bridging oxygen elimination behavior, which results in decreased glass dissolution and thus antibacterial effect.

ACKNOWLEDGMENTS

The author would like to thank Meta Bioengineering and R&D Services Inc. (Turkey) for their kind supply of Bone-G Active®. The author also would like to thank Prof. Dr. Melida Altıkatoğlu Yapaöz (Faculty of Arts & Science, Department of Chemistry, Yıldız Technical University) for her help in the antibacterial tests of the bioactive glass samples.

REFERENCES

1. Rahaman MN, Day DE, Bal BS, Fu Q, Jung SB, Bonewald LF, Tomsia AP. Bioactive glass in tissue engineering. *Acta Biomaterialia*. 2011 Jun;7(6):2355-73. Doi: 10.1016/j.actbio.2011.03.016.
2. Bellantone M, Williams HD, Hench LL. Broad-spectrum bactericidal activity of Ag₂O-doped bioactive glass. *Antimicrobial Agents and Chemotherapy*. 2020 Jun;46(6):1940-45. Doi: 10.1128/AAC.46.6.1940-1945.2002.
3. Kokubo T. Surface chemistry of bioactive glass-ceramics. *Journal of Non-Crystalline Solids*. 1990 Apr;120(1-3):138-51. Doi: 10.1016/0022-3093(90)90199-V.
4. Fernandes JS, Gentile P, Pires RA, Reis RL, Hatton PV. Multifunctional bioactive glass and glass-ceramic biomaterials with antibacterial properties for repair

- and regeneration of bone tissue. *Acta Biomaterialia*. 2017 Sep;59:2-11. Doi: 10.1016/j.actbio.2017.06.046.
5. Rabiee SM, Nazparvar N, Azizian M, Vashae D, Tayebi L. Effect of ion substitution on properties of bioactive glasses: A review. *Ceramics International*. 2015 Jul;41(6):7241-51. Doi: 10.1016/j.ceramint.2015.02.140.
6. Gerhardt LC, Boccaccini AR. Bioactive glass and glass-ceramic scaffolds for bone tissue engineering. *Materials*. 2010 Jul; 3(7):3867-910. Doi: 10.3390/ma3073867.
7. Hu S, Chang J, Liu M, Ning C. Study on antibacterial effect of 45S5 Bioglass®. *Journal of Materials Science: Materials in Medicine*. 2009 Jan; 20(1):281-86. Doi: 10.1007/s10856-008-3564-5.
8. Abushahba F, Söderling E, Aalto-Setälä L, Sangder J, Hupa L, O Närhi T. Antibacterial properties of bioactive glass particle abraded titanium against *Streptococcus mutans*. *Biomedical Physics and Engineering Express*. 2018 Apr; 4:045002. Doi: 10.1088/2057-1976/aabee.
9. Andersson ÖH, Södergård A. Solubility and film formation of phosphate and alumina containing silicate glasses. *Journal of Non-Crystalline Solids*. 1999 Apr; 246(1-2):9-15. Doi: 10.1016/S0022-3093(99)00072-1.
10. El-Kheshen AA, Khaliifa FA, Saad EA, Elwan RL. Effect of Al₂O₃ addition on bioactivity, thermal and mechanical properties of some bioactive glasses. *Ceramics International*. 2008 Sep; 34(7):1667-73. Doi: 10.1016/j.ceramint.2007.05.016.
11. Andersson ÖH, Liu G, Karlsson KH, Niemi L, Miettinen J, Juhanoja J. *In vivo* behaviour of glasses in the SiO₂-Na₂O-CaO-P₂O₅-Al₂O₃-B₂O₃ system. *Journal of Materials Science: Materials in Medicine*. 1990 Nov; 1(4):219-27. Doi: 10.1007/BF00701080.
12. Tripathi H, Hira SK, Kumar AS, Gupta U, Manna PP, Singh SP. Structural characterization and *in vitro* bioactivity assessment of SiO₂-CaO-P₂O₅-K₂O-Al₂O₃ glass as bioactive ceramic material. *Ceramics International*. 2015 Nov; 41(9):11756-69. Doi: 10.1016/j.ceramint.2015.05.143.
13. Karakuzu-Ikizler B, Terzioglu P, Basaran-Elalmis Y, Tekerek BS, Yücel S. Role of magnesium and aluminum substitution on the structural properties and bioactivity of bioglasses synthesized from biogenic silica. *Bioactive Materials*. 2020 Mar; 5(1):66-73. Doi: 10.1016/j.bioactmat.2019.12.007.
14. Karakuzu-Ikizler B, Terzioglu P, Oduncu-Tekerek BS, Yücel S. Effect of selenium incorporation on the structure and *in vitro* bioactivity of 45S5 bioglass. *Journal of The Australian Ceramic Society*. 2020 Jun; 56(2):697-709. Doi: 10.1007/s41779-019-00388-6.
15. Kesmez O. Preparation of anti-bacterial biocomposite nanofibers fabricated by electrospinning method. *Journal of the Turkish Chemical Society Section A: Chemistry*. 2020 Feb; 7(1):125-42. Doi: 10.18596/jotcsa.590621.
16. Demir C, Süer NC, Yapaöz MA, Kebir N, Okullu SO, Kocagoz T, Eren T. Biocidal activity of ROMP-polymer coatings containing quaternary phosphonium groups. *Progress in Organic Coatings*. 2019 Oct; 135:299-305. Doi: 10.1016/j.porgcoat.2019.06.008.
17. Palantoken A, Yilmaz MS, Yapaoz MA, Tulunay EY, Eren T, Piskin S. Dual antimicrobial effects induced by hydrogel incorporated with UV-curable quaternary ammonium polyethyleneimine and AgNO₃. *Materials Science and Engineering C-Materials For Biological Applications*. 2016 Nov; 68:494-504. Doi: 10.1016/j.msec.2016.06.005.
18. Dziadek M, Zagrajczuk B, Jelen P, Olejniczak Z, Cholewa-Kowalska K. Structural variations of bioactive glasses obtained by different synthesis routes. *Ceramics International*. 2016 Oct; 42(13):14700-14709. Doi: 10.1016/j.ceramint.2016.06.095.
19. Hoppe A, Meszaros R, Stähli C, Romeis S, Schmidt J, Peukert W, Marelli B, Nazhat SN, Wondraczek L, Lao J, Jallot E, Boccaccini AR. *In vitro* reactivity of Cu doped 45S5 Bioglass® derived scaffolds for bone tissue engineering. *Journal of Materials Chemistry B*. 2013 Nov;41:5659-5674. Doi: 10.1039/c3tb21007c.
20. Lefebvre L, Chevalier J, Gremillard L, Zenati R, Thollet G, Bernache-Assolant D, Govin A. Structural transformations of bioactive glass 45S5 with thermal treatments. *Acta Materialia*. 2007 Jun;55(10):3305-3313. Doi: 10.1016/j.actamat.2007.01.029.
21. Romeis S, Hoppe A, Eisermann C, Schneider N, Boccaccini AR, Schmidt J, Peukert W. Enhancing *in vitro* bioactivity of melt-derived 45S5 Bioglass® by comminution in a stirred media mill. *Journal of the American Ceramic Society*. 2014 Jan;97(1):150-156. Doi: 10.1111/jace.12615.
22. Sepulveda P, Jones JR, Hench LL. *In vitro* dissolution of melt-derived 45S5 and sol-gel derived 58S bioactive glasses. *Journal of Biomedical Materials Research*. 2002 Aug;61(2):301-311. Doi: 10.1002/jbm.10207.
23. Gorriti MF, López JMP, Boccaccini AR, Audisio C, Gorustovich AA. *In vitro* study of the antibacterial activity of bioactive glass-ceramic scaffolds. *Advanced Engineering Materials*. 2009 Jul;11(7):B67-B70. Doi: 10.1002/adem.200900081.
24. Zhang D, Leppäranta O, Munukka E, Ylänen H, Viljanen MK, Eerola E, Hupa M, Hupa L. Antibacterial effects and dissolution behavior of six bioactive glasses. *Journal of Biomedical Materials Research*

Part A. 2010 May;93A(2):475-483. Doi: 10.1002/jbm.a.32564.

25. Allan I, Newman H, Wilson M. Antibacterial activity of particulate Bioglass® against supra-and subgingival bacteria. *Biomaterials*. 2001 Jun;22(12):1683-1687. Doi: 10.1016/S0142-9612(00)00330-6.

26. Leppäranta O, Vaahtio M, Peltola T, Zhang D, Hupa L, Hupa M, Ylänen H, Salonen JI, Viljanen MK, Eerola E. Antibacterial effect of bioactive glasses on clinically important anaerobic bacteria *in vitro*. *Journal of Materials Science: Materials in Medicine*. 2008 Feb;19(2):547-551. Doi: 10.1007/s10856-007-3018-5.

